Virtual Screening: A Step Towards a Sparse Partial Inductance Matrix

A. J. Dammers[1,2] and N. P. van der Meijs[1]

[1] Delft Institute of Microelectronics and Submicron Technology
Department of Electrical Engineering, Circuits and Systems Section
Delft University of Technology, P.O. Box 5031, 2600 GA Delft (NL)

[2]Netherlands Institute for Metals Research and Delft University of Technology
Department of Materials Science, Rotterdamseweg 137, 2628 AL Delft (NL)

Abstract

We extend the partial inductance concept by replacing the magnetic interaction between open filaments i and j by that between filament j and a (finite) closed loop, formed by connecting the endpoints of a filament pair (i-i'). The secondary filament i' is constructed by radial projection of filament i onto a cylindrical shell around filament j. We show that, although individual partial inductance values are modified, the inductive behaviour of the full circuit is invariant. Mutual inductances of distant filaments are particularly reduced, because the far field of a conductor loop falls off much faster than that of a single filament. Therefore, it is expected that subsequent removal of such transformed off-diagonal elements from the partial inductance matrix has less effect on the overall inductive properties, so our method provides a tool to enhance robustness under matrix sparsification. We call our method "virtual screening", because the screening filaments $\{i'\}$ are not physically present. Symmetry of the inductance matrix is preserved for orthogonal networks only.

We also present an extension of our method to a more general class of shells. This allows a detailed comparison of the virtual screening method and the "potential shift-truncate method", introduced with spherical equipotential shells [Krauter et al. ICCAD'95] and extended to ellipsoidal equipotential shells recently [Beattie et al. IEDM'98]. We find strong similarities, but also differences. An interesting result is the fact that the virtual screening method with tubular shells applied to orthogonal networks can be interpreted as a generalization of the potential shift-truncate method to non-equipotential shells, which also implies that preservation of stability is guaranteed.

Some numerical results, sustaining the ideas behind our method, conclude the paper.

1 Introduction

In deep submicron technology feature sizes decrease, clock speeds get higher and chips get larger and more complex. Therefore, parasitic inductive effects in on-chip interconnects are playing an increasingly important role. The high degree of complexity of the circuits renders the modelling of such phenomena a non-trivial task. Current paths may be rather erratic, depending on the details of the signals present. This implies that description of inductive effects in terms of well-defined simple geometric structures is ruled out beforehand.

Layout-to-circuit extraction aims at transforming the physical description of an integrated circuit to a highly reduced electrical lumped circuit representation, which may subsequently be handled by circuit simulators such as SPICE. This objective is at first sight incompatible with the distributed character of inductive phenomena, as self and mutual inductances are defined for closed current loops only, and these may span a major part of a circuit. The partial inductance concept [1] provides a handle to this problem. Unclosed conductor segments can formally be treated as magnetically coupled lumped circuit elements. The practical problem, however, is the fact that this results in networks with a high degree of connectivity. This implies that the associated partial inductance matrix is densely filled, which strongly diminishes the efficiency of numerical methods which have proven to be useful for *RC*-problems.

The most efficient method applied thus far for reduction of a system of partial inductances to a reduced (smaller) one is GMRES with multipole acceleration, as implemented in FastHenry [2]. This method is, however, in its present form far too slow to be useful for full circuits, which may comprise up to well over one million transistors. Attempts to sparsify the inductance matrix by merely discarding relatively small elements often has an unacceptable effect on the circuit properties, and may even lead to loss of passivity.

We analyse the latter problem from a conceptual point of view, starting from the interpretation [1] of partial inductances in terms of magnetic flux enclosed by loops extending from conductor segments to infinity. The method we develop in this paper replaces such loops by finite ones, without modifying the inductive behaviour of the full circuit. Such finite loops are formed by assuming that the current induced in filament *i* by that in filament *j* has a return path on a cylindrical shell around filament *j*, rather than at infinity. This is reminiscent of the "potential shift-truncate method" [3] [4], where an equipotential shell around a filament screens its magnetic vector potential.

0-7803-5832-X /99/$10.00 ©1999 IEEE.

Our method, although derived with a cylindrical shell, allows the use of *any* shell with axial symmetry. This includes the equipotential shells mentioned above, as these are rotational ellipsoids. This raises the question whether an equipotential shell has a special status. Furthermore, the interpretation of the potential shift-truncate method in terms of shell currents appears to be quite different from the model which arises from our construction. In order to deal with these issues, we present an alternative derivation of our method, which reveals the connection with the potential shift-truncate method in an unambiguous way.

In Sec. 2 we summarize key aspects of the partial inductance concept, as far as these are relevant in this paper. In Sec. 3 a modified partial inductance matrix is constructed, using a cylindrical shell. Invariance of the overall inductive behaviour is proven and issues concerning the practical application of the transformation are discussed. In Sec. 4 the same results are obtained starting from a gauge transformation of the vector potential generated by a current element. We derive expressions for cylinders, as well as ellipsoidal equipotential shells. Using these results, the potential shift-truncate method and its connection with the virtual screening approach is analysed in Sec. 5.

A simple transmission line model is analysed numerically in Sec. 6, in order to illustrate the ideas underlying our method.

2 Flux related issues of the PEEC approach

2.1 Interpretation of partial inductance elements

In the magnetoquasistatic regime the inductive properties of a circuit can be formulated [1] in terms of the interaction between conductor segments carrying uniform current densities. These segments are building blocks of the full conductors. The coupling between such segments is characterized by *partial inductances*

$$L_{ij}^{(p)} = \frac{1}{I_j} \left| \int_a^b \mathbf{A}_{ij} \cdot d\mathbf{l}_i \right| , \tag{1}$$

where $\mathbf{A}_{ij}$ represents the vector potential due to current $\mathbf{I}_j$ in segment j, at some length coordinate $\mathbf{l}_i$ on segment i, averaged over its cross section a_i. This may be written in a more symmetric form in terms of the magnetic interaction of infinitesimally thin *filaments*, averaged over the cross sections of segments i and j respectively:

$$L_{ij}^{(p)} = \frac{1}{a_i a_j} \iint da_i da_j \left\{ \frac{\mu_0}{4\pi} \iint \frac{\left| d\mathbf{l}_i \cdot d\mathbf{l}_j \right|}{\left| \mathbf{r}_i - \mathbf{r}_j \right|} \right\} , \tag{2}$$

where $\mathbf{r}_i$ and $\mathbf{r}_j$ are the position vectors of infinitesimal filaments $d\mathbf{l}_i$ and $d\mathbf{l}_j$. Without loss of generality we continue our discussion for filaments only, because the procedure developed in this paper amounts to replacing $\{\dots\}$ by a linear combination of such terms.

Ruehli [1] relates the partial inductance which characterizes interaction between unclosed conductor filaments to the magnetic flux enclosed by a *loop* which extends from a conductor filament to infinity. We summarize this interpretation, as it forms the basis for our introduction of a modified partial inductance matrix. Such a construction is visualized in Fig. 1.

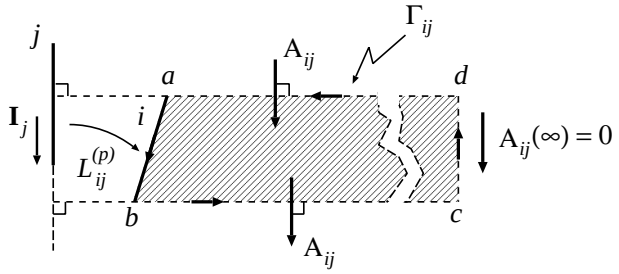

Figure 1: **The partial inductance $L_{ij}^{(p)}$ between filaments i and j is related to the magnetic flux due to current $\mathbf{I}_j$ bounded by the contour Γ_{ij}, visualized as a shaded area. [1]**

Filament i is supplemented by filaments extending from its end points to infinity, perpendicular to filament j. A closed loop Γ_{ij} is formed by connecting the endpoints of these filaments at infinity (in an arbitrary manner). This geometric construction applies to any pair of, possibly *non-coplanar*, filaments i and j. The line integral in (1) may be related to the contour integral along Γ_{ij} by considering the enclosed magnetic flux

$$\Psi_{\Gamma_{ij}} = \oint_{\Gamma_{ij}} \mathbf{A}_{ij} \cdot d\mathbf{l} , \tag{3}$$

where now $\mathbf{A}_{ij}$ is understood to be the vector potential at any point along Γ_{ij} due to current $\mathbf{I}_j$. This contour integral is decomposed into integrals along filaments as

$$\oint_{\Gamma_{ij}} = \int_a^b + \underbrace{\int_b^c}_{0} + \underbrace{\int_c^d}_{0} + \underbrace{\int_d^a}_{0} \rightarrow \int_a^b . \tag{4}$$

The last three line integrals give no contribution, because $\mathbf{A}_{ij} \perp d\mathbf{l}$ on bc and da, and $\mathbf{A}_{ij} = 0$ on cd. A partial inductance related to this enclosed flux is defined as

$$L_{\Gamma_{ij}}^{(p)} = \frac{1}{I_j} \left| \Psi_{\Gamma_{ij}} \right| = \frac{1}{I_j} \left| \oint_{\Gamma_{ij}} \mathbf{A}_{ij} \cdot d\mathbf{l} \right| . \tag{5}$$

With (4) we see that (5) reduces to (1), so

$$L_{ij}^{(p)} = L_{\Gamma_{ij}}^{(p)} . \tag{6}$$

2.2 Sparsification of the partial inductance matrix

The sparsity of the partial inductance matrix $\mathbb{L}$ may be increased by discarding some small (off-diagonal) elements. However, it is known that this may have a substantial effect on the overall inductive behaviour, and may even result in loss of passivity. The flux interpretation of partial inductances enables us to appreciate this in a more intuitive way. Consider a closed loop Γ carrying current I (Fig. 2). The self inductance L of this loop is related to its enclosed magnetic flux Ψ_Γ by $L = |\Psi_\Gamma| / I$. Alternatively, L can be written in terms of partial inductances $\{L_{ij}^{(p)}\}$, which are related to fluxes $\{\Psi_{\Gamma_{ij}}\}$ penetrating surface areas bounded by contours $\{\Gamma_{ij}\}$, extending from the filaments $\{i\}$ to infinity (Fig. 1):

$$L = \left| \sum_{i,j} s_{ij} L_{ij}^{(p)} \right| = \left| \sum_{i,j} \frac{1}{I_j} \Psi_{\Gamma_{ij}} \right| , \tag{7}$$

where $s_{ij} \equiv \mathrm{sign}(\mathbf{A}_{ij} \cdot d\mathbf{l}_j)$. The sizes of the shaded areas in Fig. 2b

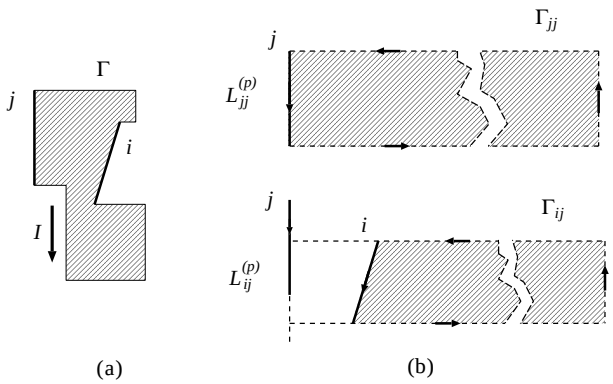

Figure 2: **(a) The self inductance L of the closed current loop Γ is proportional to the magnetic flux penetrating the surface area enclosed by this loop. (b) The partial inductances which form the overall inductance are related to fluxes penetrating surface areas extending from the current filaments to infinity (see Fig. 1).**

compared to that in Fig. 2a suggest that large fractions of the partial inductances should cancel upon performing the summation (7). This observation may be used to explain the effect of truncation of the partial inductance matrix. Discarding an off-diagonal element $L_{ij}^{(p)}$ of L implies that $\Psi_{\Gamma_{ij}}$ is no longer taken into account. On the other hand, the terms which otherwise would take care of the compensation of this flux will still be present in (7). Consequently the energy balance is disturbed and the system may even manifest itself as non-passive.

3 Modification of partial inductances

The qualitative analysis of the effect of matrix sparsification on inductive behaviour (Sec. 2.2) suggests that an important error source is related to magnetic flux implied in the partial inductance definition, but which is *external* to the area enclosed by the circuit. This inspired us to investigate the possibility to truncate the magnetic flux generated by a current filament external to a cylindrical shell around it. First, we will formulate the basic principle of the construction of modified partial inductances which represent such truncated fluxes. For reasons of clarity this is restricted to the case of coplanar conductor filaments. Then we will show how the construction can be generalized for filaments at any relative (non-planar) orientation. Subsequently we will prove that indeed flux truncation may be carried out without modifying the physical properties of the system. This section is concluded by a discussion on the physical interpretation of our method and some comments on criteria guiding the choice of the cylinder size.

3.1 Construction

Consider two coplanar filaments i and j at arbitrary relative orientation. With the flux interpretation their partial mutual inductance can be written as (see (5) and (6))

$$L_{ij}^{(p)} = \frac{1}{I_j} \left| \oint_{\Gamma_{ij}} \mathbf{A} \cdot d\mathbf{l} \right| , \tag{8}$$

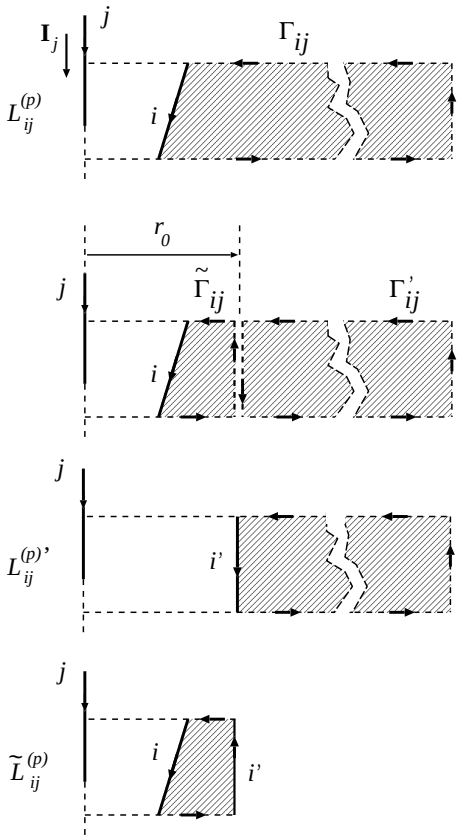

Figure 3: **Modification of partial inductance.**

where $\mathbf{A}$ is understood to be the magnetic vector potential due to current $\mathbf{I}_j$ (indices are omitted for brevity). The area bounded by Γ_{ij} is divided into two regions by a line parallel to filament j and separated from it by a distance r_0 (Fig. 3). The two subareas are enclosed by $\tilde{\Gamma}_{ij}$ and Γ'_{ij} respectively. Accordingly, the contour integral in (8) is written as

$$\oint_{\Gamma_{ij}} = \oint_{\tilde{\Gamma}_{ij}} + \oint_{\Gamma'_{ij}} . \tag{9}$$

$\tilde{\Gamma}_{ij}$ and Γ'_{ij} share a filament, which is labeled i'. The respective contributions of i' to the integration cancel because $\tilde{\Gamma}_{ij}$ and Γ'_{ij} traverse i' in opposite directions. We relate the flux enclosed by Γ'_{ij} to the partial inductance

$$L_{ij}^{(p)\prime} \equiv L_{i'j}^{(p)} = \frac{1}{I_j} \left| \oint_{\Gamma'_{ij}} \mathbf{A} \cdot d\mathbf{l} \right| \tag{10}$$

between filament j and *virtual* filament i'. Likewise we *formally* write

$$\tilde{L}_{ij}^{(p)} = \frac{1}{I_j} \left| \oint_{\tilde{\Gamma}_{ij}} \mathbf{A} \cdot d\mathbf{l} \right| . \tag{11}$$

or alternatively

$$\tilde{L}_{ij}^{(p)} = L_{ij}^{(p)} - L_{ij}^{(p)\prime} . \tag{12}$$

The planar construction is readily generalized to the non-planar case by defining a cylindrical shell with radius r_0 around

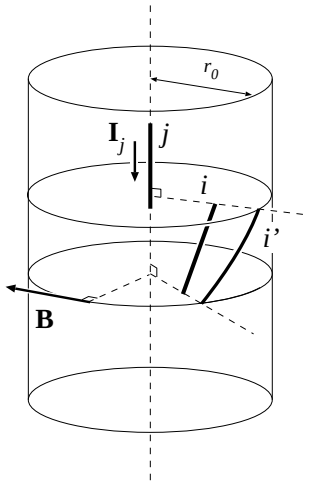

Figure 4: **A cylinder with radius r_0 is centered around filament j. The flux area associated with L_{ij} (Fig. 1) extends from filament i to infinity. The intersection curve of this surface with the cylindrical shell is i'.**

filament j. The flux area related to $L_{ij}^{(p)}$ is a twisted surface. Its intersection curve i' with the cylinder is *not* a straight line (Fig. 4). The formal construction of $\tilde{L}_{ij}^{(p)}$ follows the same arguments as in the coplanar case.

3.2 Equivalence of $L_{ij}^{(p)}$ and $\tilde{L}_{ij}^{(p)}$

Filament i will always be part of a closed current loop, say Γ_c, as such loops are the only physically valid structures. The magnetic flux due to current $\mathbf{I}_j$ enclosed by Γ_c is

$$\Psi_{\Gamma_c j} = \oint_{\Gamma_c} \mathbf{A}\cdot d\mathbf{l} = I_j \sum_{i\in\Gamma_c} s_{ij} L_{ij}^{(p)} \,. \tag{13}$$

According to (9) the contour integral is split into contributions relating to $\tilde{L}_{ij}^{(p)}$ and $L_{ij}^{(p)\prime}$ respectively:

$$\Psi_{\Gamma_c j} = \sum_i \oint_{\Gamma_{ij}} \mathbf{A}\cdot d\mathbf{l} = \sum_i \oint_{\tilde{\Gamma}_{ij}} \mathbf{A}\cdot d\mathbf{l} + \sum_i \oint_{\Gamma'_{ij}} \mathbf{A}\cdot d\mathbf{l} \,. \tag{14}$$

The second term on the right-hand side is recast as

$$\sum_i \oint_{\Gamma'_{ij}} \mathbf{A}\cdot d\mathbf{l} = \sum_i \int_{l'_i} \mathbf{A}\cdot d\mathbf{l} = \oint_{\Gamma'_c} \mathbf{A}\cdot d\mathbf{l} \,, \tag{15}$$

where Γ'_c is a *closed* loop on the cylinder surface (radial projection of Γ_c) consisting of filaments $\{l'_i\}$. These filaments are in general not linear (see below). Because the magnetic field $\mathbf{B}$ due to current $\mathbf{I}_j$ is *tangential* to the cylinder we have

$$\oint_{\Gamma'_c} \mathbf{A}\cdot d\mathbf{l} = \int\int \mathbf{B}\cdot d\mathbf{S} \equiv 0 \,, \tag{16}$$

so (14) reduces to

$$\Psi_{\Gamma_c j} = \sum_i \oint_{\tilde{\Gamma}_{ij}} \mathbf{A}\cdot d\mathbf{l} = I_j \sum_i s_{ij} \tilde{L}_{ij}^{(p)} \,. \tag{17}$$

This expression may also be obtained from (13) by substituting

$$L_{ij}^{(p)} \to \tilde{L}_{ij}^{(p)} \,. \tag{18}$$

As the electrical behaviour is invariant under this operation, we conclude that $\{\tilde{L}_{ij}^{(p)}\}$ and $\{L_{ij}^{(p)}\}$ yield equivalent descriptions for the full network.

3.3 Computation of $\tilde{L}_{ij}^{(p)}$ in terms of parallel linear filaments

The intersection filament i' of the flux surface related to $L_{ij}^{(p)}$ and the cylinder with radius r_0 around filament j is in general not a straight line. This presents us with a problem, as we need to calculate $L_{ij}^{(p)\prime}$, the partial mutual inductance between j and i'. However, we will show that it can be related to the partial inductance between j and a *linear* filament i'' on the cylinder, parallel to j and characterized further by

$$\mathbf{l}_{i''} = (\mathbf{l}_i \cdot \hat{\mathbf{l}}_j)\hat{\mathbf{l}}_j \,, \tag{19}$$

where $\hat{\mathbf{l}}_j \equiv \mathbf{l}_j / l_j$. Filaments i' and i'' share one endpoint and by

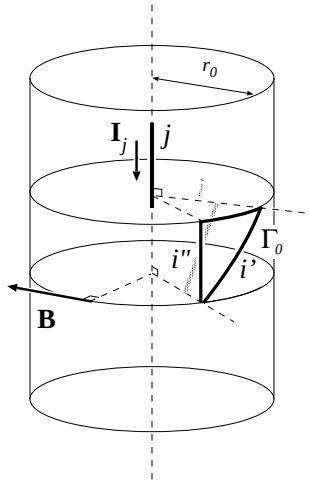

Figure 5: **A triangular network Γ_0 on the cylinder is used to prove the equivalence of the magnetic coupling of filament j with filaments i' and i'' respectively.**

connecting the opposite endpoints by a circular arc on the cylinder a closed circuit Γ_0 is formed (Fig. 5). As argued previously (see (16)) filament j and any closed loop on the cylindrical shell are uncoupled, so

$$\oint_{\Gamma_0} \mathbf{A}\cdot d\mathbf{l} = 0 \,. \tag{20}$$

Because the circular arc which connects i' and i'' is perpendicular to $\mathbf{l}_j$, its contribution to the contour integral is zero, so

$$\oint_{\Gamma_0} \mathbf{A}\cdot d\mathbf{l} \;\to\; \int_{i'} \mathbf{A}\cdot d\mathbf{l} + \int_{i''} \mathbf{A}\cdot d\mathbf{l} = 0 \,, \tag{21}$$

and therefore $\int_{i'} \mathbf{A}\cdot d\mathbf{l} = -\int_{i''} \mathbf{A}\cdot d\mathbf{l}$. Thus we conclude

$$L_{i'j}^{(p)} = L_{i''j}^{(p)} \tag{22}$$

and with a change in notation $L_{ij}^{(p)\prime\prime} \equiv L_{i''j}^{(p)}$ we arrive at the final result

$$\tilde{L}_{ij}^{(p)} = L_{ij}^{(p)} - L_{ij}^{(p)\prime\prime} \,. \tag{23}$$

For the calculation of $L_{ij}^{(p)\prime\prime}$, the partial mutual inductance of two parallel filaments, exact expressions are available [5].

Because of space limitations we will just state important constraints of the method, without presenting the derivation: symmetry of $\tilde{\mathsf{L}}$ will only be preserved for *orthogonal* networks, provided that unique screening radii $r_0^{(x)}$, $r_0^{(y)}$ and $r_0^{(z)}$ are chosen for filaments in the three principal directions respectively. Details can be found in [6].

3.4 Discussion

Virtual screening

The transformation $L_{ij}^{(p)} \to \tilde{L}_{ij}^{(p)}$ is interpreted (Fig. 3) in terms of a return path i' for the current induced in filament i. The return current effectively screens the interaction with filament j. As filament i' is not physically present, we refer to our method as *virtual screening*. A complementary view of the screening effect is obtained by noting that essentially partial inductances (2) represent interactions between "monopoles" (unclosed filaments), which are strictly mathematical, rather than physical, objects. Augmenting filament i by a virtual return filament i' replaces i by a finite closed loop, which gives its (far) field a more dipole-like character. Hence the interaction with filament j is reduced. Therfore, our method is expected to provide a tool which enhances robustness under sparsification of the inductance matrix.

Choice of r_0

The formal construction of $\tilde{L}_{ij}^{(p)}$ does not restrict the value of the cylinder radius r_0. Suppose we reduce r_0 such that $\tilde{L}_{ij}^{(p)} = 0$ (filament i and the cylinder intersect). We then have a representation where filaments j and i are effectively decoupled (a numerical illustration appears in Sec. 6). This suggests that in practical applications one would choose r_0 such, that the cylinder extends to the most distant conductor in the network. However, in a carefully designed circuit long distance couplings between signal lines will be considerably reduced by the presence of nearby (physical) current return paths. Therefore, reduction of the cylinder to a size which encloses all *relevant* conductors would be optimal. This would render some elements of $\tilde{\mathsf{L}}$ negative, but these can be set to zero, as they represent irrelevant couplings which have no significant effect on the overall circuit behaviour. In fact, if we know, from geometric considerations, that filament i is excluded from the cylinder completely, computation of the associated matrix element is not necessary, because it will be negative and thus set to zero eventually. The optimal cylinder radius r_0 depends on the inductive and resistive properties of the network in combination with the signal frequency. Discussions relevant to this issue can be found in references [3] and [4], where a method closely related to our virtual screening approach is discussed (see Sec. 5).

4 Generalization to non-cylindrical shells

The procedure followed in sections 3.1 and 3.2 may be applied to *any* surface with axial symmetry. The symmetry requirement is necessary in view of (16). An alternative route to the same results is obtained through the application of a *gauge transformation* [7] to the vector potential $\mathbf{A}_j$. We give an account of this approach, as it clarifies the physical background of our method. Moreover, it provides a bridge to the potential shift-truncate method [3] [4], which will be analysed in Sec. 5.

4.1 General procedure

Gauge transformation of $\mathbf{A}_j$

In the magnetoquasistatic regime an electromagnetic system is invariant under a *gauge transformation* [7] of the vector potential

$$\mathbf{A} \to \tilde{\mathbf{A}} \equiv \mathbf{A} - \mathbf{A}' \,, \tag{24}$$

where $\mathbf{A}'$ is *irrotational*, i.e.

$$\nabla \times \mathbf{A}' = 0 \,, \tag{25}$$

which ensures invariance of the magnetic field $\mathbf{B} = \nabla \times \mathbf{A}$. If we apply this procedure to the vector potential $\mathbf{A}_j$, generated by a current in filament j, it should leave the overall inductive behaviour of the circuit unaltered. This implies that the modified partial inductance matrix $\tilde{\mathsf{L}}$ with elements

$$\tilde{L}_{ij}^{(p)} = \frac{1}{I_j} \left| \int_i \tilde{\mathbf{A}}_j \cdot d\mathbf{l} \right| \tag{26}$$

represents the *same* physical system as the original matrix L. The relation between this transformation and the virtual screening method can be readily established by considering the analogue of Fig. 1 for $\tilde{L}_{ij}^{(p)}$. The closing filament must now be chosen such that $\tilde{\mathbf{A}}_j = 0$, i.e. it lies on a surface defined implicitly by $\mathbf{A}_j = \mathbf{A}'_j$. In other words, the (zero) reference potential is shifted from infinity to a finite distance. This interpretation is consistent with the geometric construction in Fig. 3.

Symmetry of $\mathbf{A}'_j$

The magnetic vector potential $\mathbf{A}_j$, related to a current $\mathbf{I}_j = I_j \hat{\mathbf{l}}_j$ in filament j, is parallel to $\mathbf{I}_j$ and has axial symmetry, i.e.

$$\mathbf{A}_j = A_j(r,z)\,\hat{\mathbf{l}}_j \,, \tag{27}$$

where r and z are the radial an longitudinal coordinates respectively. An obvious choice would be to require that $\tilde{\mathbf{A}}_j$ has the same symmetry properties as $\mathbf{A}_j$, which implies

$$\mathbf{A}'_j = A'_j(r,z)\,\hat{\mathbf{l}}_j \,. \tag{28}$$

However,

$$\nabla \times \mathbf{A}'_j = \nabla A'_j(r,z) \times \hat{\mathbf{l}}_j \; = -r \left(\frac{\partial A'_{j,z}}{\partial r} \right) \mathbf{e}_\phi, \tag{29}$$

where $\mathbf{e}_\phi$ is the azimuthal unit vector in the cylindrical coordinate system (r,ϕ,z). Therefore, condition (25) can only be met if

$$\mathbf{A}'_j = A'_j(z)\,\hat{\mathbf{l}}_j \,, \tag{30}$$

i.e. $\mathbf{A}'_j$ is constant in planes perpendicular to $\mathbf{I}_j$.

4.2 Specific shells

Cylindrical shell

We relate $\mathbf{A}'_j$ to the value of $\mathbf{A}_j$ on the cylinder $r = r_0$, i.e.

$$\mathbf{A}'_j = A_j(r_0,z)\,\hat{\mathbf{l}}_j\,, \tag{31}$$

which is consistent with requirement (30).
Referring to the geometry of Fig. 5 this implies

$$\begin{aligned}\int_i \mathbf{A}'_j\cdot d\mathbf{l} &= \int_i A_j(r_0,z)\,(\hat{\mathbf{l}}_j\cdot\hat{\mathbf{l}}_i)\,dz \\ &= \int_{i''} A_j(r_0,z)\,dz = \int_{i''}\mathbf{A}_j\cdot d\mathbf{l}\,. \end{aligned}\tag{32}$$

Hence (premultiply by $1/I_j$) we obtain

$$\tilde{L}^{(p)}_{ij} = L^{(p)}_{ij} - L^{(p)}_{i''j}\,. \tag{33}$$

This is equivalent to (23).

Ellipsoidal equipotential shell

The key ingredients of the potential shift-truncate method [3] [4] (see Sec. 5) are (ellipsoidal) equipotential shells around filaments. Such equipotential shells may be related to the virtual screening framework by requiring that the gauge potential $\mathbf{A}'_j$ is constant, i.e.

$$\mathbf{A}'_j(z) = \mathbf{A}_j(r,z)\big|_{A_j=A_{0,j}} = A_{0,j}\,\hat{\mathbf{l}}_j\,. \tag{34}$$

The equipotential surfaces $A_j(r,z) = A_{0,j}$ are rotational ellipsoids [4]. Integration of $\mathbf{A}'_j$ along segment i gives

$$\begin{aligned}\int_i \mathbf{A}'_j\cdot d\mathbf{l} &= \int_i A_{0,j}\hat{\mathbf{l}}_j\cdot d\mathbf{l} \\ &= A_{0,j}\int_i (\hat{\mathbf{l}}_j\cdot\hat{\mathbf{l}}_i)\,dz = A_{0,j}\,l_i\,(\hat{\mathbf{l}}_i\cdot\hat{\mathbf{l}}_j)\,. \end{aligned}\tag{35}$$

Then (normalize $\mathbf{A}_j$ to $I_j = 1$) the modified partial inductance (26) is given by

$$\tilde{L}^{(p)}_{ij} = L^{(p)}_{ij} - A_{0,j}l_i\,\big|\hat{\mathbf{l}}_i\cdot\hat{\mathbf{l}}_j\big|\,. \tag{36}$$

The equivalent expression of $\tilde{L}^{(p)}_{ij}$ in [4] is obtained by identifying $|\hat{\mathbf{l}}_i\cdot\hat{\mathbf{l}}_j| = \cos\alpha_{ij}$. A convenient choice for the potential parameter, suggested in [4], is

$$A_{0,j} = \kappa l_j\,. \tag{37}$$

This preserves symmetry of the partial inductance matrix, as is clear from

$$\tilde{L}^{(p)}_{ij} = L^{(p)}_{ij} - \kappa|\mathbf{l}_i\cdot\mathbf{l}_j|\,. \tag{38}$$

5 The potential shift - truncate method

5.1 General description

In the potential shift-truncate method [3] [4] interactions of filament j with parts of the circuit external to an equipotential shell around j, defined by $\mathbf{A}_j(\mathbf{r}) = \mathbf{A}_{0,j}$, are discarded. This amounts to introducing a truncated vector potential

$$\overline{\mathbf{A}}_j(\mathbf{r}) = \Theta_j(\mathbf{r};A_{0,j})\;\tilde{\mathbf{A}}_j(\mathbf{r})\,, \tag{39}$$

where the step function Θ_j is defined as

$$\Theta_j(\mathbf{r};A_{0,j}) = \begin{cases} 1 & , \quad A_j \geq A_{0,j} \\ 0 & , \quad A_j < A_{0,j} \end{cases}\,. \tag{40}$$

$\tilde{\mathbf{A}}_j(\mathbf{r})$ is the vector potential constructed from $\mathbf{A}_j(\mathbf{r})$ through a gauge transformation, as discussed in Sec. 4.2. Accordingly, associated partial inductances are obtained as

$$\overline{L}^{(p)}_{ij} = \frac{1}{I_j}\left|\int_i \overline{\mathbf{A}}_j\cdot d\mathbf{l}\right|\,. \tag{41}$$

When the equipotential shell of filament j encloses filament i completely, we have $\overline{L}^{(p)}_{ij} = \tilde{L}^{(p)}_{ij}$, which is the virtual screening result. When filament i is completely outside of the shell we have $\overline{L}^{(p)}_{ij} = 0$, whereas $\tilde{L}^{(p)}_{ij} < 0$, but in the postprocessing step of our method, as discussed in Sec. 3.4, we would set such a negative matrix element equal to zero, so again identical results are obtained. When filament i intersects the shell, however, the two methods are different. The potential shift-truncate method then effectively calculates $\overline{L}^{(p)}_{ij}$ as the mutual inductance between filament j and a *physically truncated* filament i. It was shown in [3] that this procedure, effectuated by a current distributed over the shell, which represents the (imaginary) return current of that in filament j, guarantees a positive semidefinite modified inductance matrix. In our virtual screening approach, however, we account for the interaction of filament j and the *full* filament i. When in the postprocessing step of matrix $\tilde{\mathrm{L}}$ the negative matrix elements are discarded, loss of stability does not seem to be excluded beforehand. However, if either method is to be used as a preprocessing step for improved robustness of the matrix under sparsification, this difference will diminish.

An interesting observation at this point is the fact that for tubular shells applied to orthogonal networks, filaments and shells will never intersect. Although such cylinders are not equipotential shells, we could follow the same arguments as in [3] and arrive at the conclusion that also here stability is guaranteed.

5.2 Geometric considerations

The equipotential surfaces employed in the potential shift-truncate method are rotational ellipsoids

$$(z/z_0)^2 + (r/\rho_0)^2 = 1\,, \tag{42}$$

where the semi axes ρ_0 and z_0 are functions of $A_{0,j}$ and l_j. From the explicit expressions given in [4] the potential parameter $A_{0,j}$ can be eliminated. This gives

$$z_0^2 = \rho_0^2 + (l_j/2)^2\,. \tag{43}$$

When $\rho_0 \gg l_j$ we have $z_0 \approx \rho_0$, so the shell is essentially spherical. The other limit $\rho_0 \ll l_j$ gives $z_0 \approx l_j/2$, i.e. the ellipsoid closely "wraps" the filament. A general consequence of (43) is, that z_0 is fixed for a given choice of ρ_0.

This observation suggests that for orthogonal networks tubular shells may be more suitable, because these are open in the z-direction.

6 Numerical example

We consider the partial inductance formulation of a transmission line system (Fig. 6) consisting of two parallel wires (rectangular cross sections) of length l, carrying currents which are equal in magnitude, but in opposite direction. The geometric (dimensionless) parameters used are: $W = T = 1$, $l = 400$, $d = 5$, $\lambda = 20$. Partial self inductances are calculated using an exact expression, whereas for mutual inductances we approximated the conductors by single filaments [1].

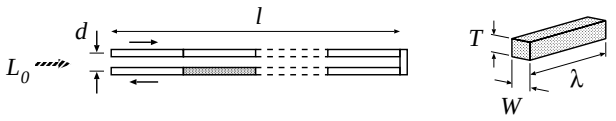

Figure 6: **Transmission line consisting of two parallel conductors with rectangular cross sections.**

For a particular choice of the screening radius r_0 the inductance matrix $\tilde{\mathrm{L}}$ is generated. The inductance L_0 of the circuit calculated from $\tilde{\mathrm{L}}$ is independent of r_0. End segments, which close the circuit, are disregarded. This can be justified by the fact that essentially they are perpendicular to the segments considered here, or even simpler because their contribution is small. Subsequently a series of degrees of sparsity of the matrix is created by setting all elements below some threshold value to zero, and the resulting network inductance L is calculated. This truncation procedure is repeated for increasingly higher thresholds, resulting in higher sparsity. The resulting behaviour of L/L_0 is given in Fig. 7. In Fig. 7a, which represents the behaviour of the unmodified inductance matrix ($r_0 \to \infty$), two branches can be recognized, one dominantly constant at a level $L/L_0 \approx 1$, and one which increases with sparsity. The constant branch corresponds to configurations where facing segment *pairs*, carrying opposite currents, are discarded (their corresponding matrix elements are removed from $\tilde{\mathrm{L}}$). Their spacing is such that the magnetic coupling with segments further along the line is effectively screened. When only *one* segment of a pair is removed, its counterpart is left unscreened, which manifests itself as a significant additional contribution to L. The latter category constitutes the second branch, which exhibits an increase of L/L_0 with sparsity. When r_0 is given a finite value (Fig. 7b), the effect of leaving one member of a conductor pair uncompensated diminishes, which is the goal of the virtual screening method. The optimal situation occurs when r_0 is equal to the conductor spacing d (Fig. 7c), as the "mathematical" segment pairs underlying $\tilde{\mathrm{L}}$ and the physical ones then coincide. Effectively, the two sets of branches are then decoupled, as discussed in Sec. 3.4. Consequently, the matrix is block-diagonal, which explains why the sparsity in Fig. 7c has a minimum value of 50%.

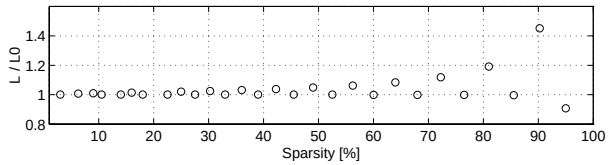

(a) No screening ($r_0 \to \infty$)

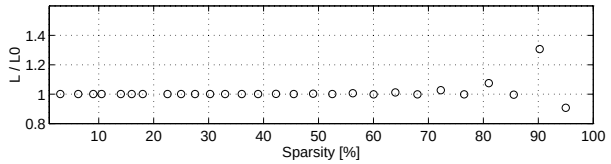

(b) $r_0 = 50$

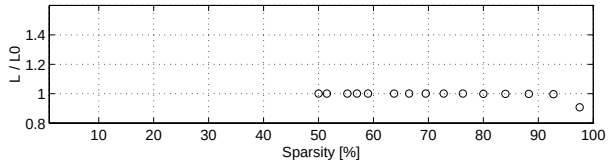

(c) $r_0 = 5$

Figure 7: **Behaviour of the normalized inductance L/L_0 upon truncation of $\tilde{\mathrm{L}}$, for values of the screening radius: (a) $r_0 \to \infty$, (b) $r_0 = 50$ and (c) $r_0 = 5$.**

7 Conclusions

We have derived a "virtual screening" method, which amounts to augmenting a filament i, in which a current is induced by filament j, with a filament i' on a cylindrical shell around j. Filament i' carries the return current of that in i. The procedure changes individual partial inductances, but has no influence on the overall circuit behaviour. It is expected to diminish the effect of sparsification of the inductance matrix. This was sustained by some numerical experiments.

We generalized our method to arbitrary shells with axial symmetry. This allowed us to compare our results with the closely related potential shift-truncate method. Our conclusion is, that the virtual screening method, followed by removal of negative matrix elements, approximately recovers the same results. Differences occur, because in the potential shift-truncate method a filament intersecting a shell is explicitly truncated, whereas in the virtual screening approach we first calculate the interaction with the full filament and then, if the result is negative, it is discarded. As the physical truncation of filaments is implied in the proof of the fact that the potential shift-truncate method maintains a positive semidefinite inductance matrix, this property may possibly be lost in our approach. On the other hand, when cylindrical shells are utilized for orthogonal networks, filament truncation will not occur. Our virtual screening approach can then be interpreted as a generalization of the potential shift-truncate method to *non-equipotential* shells, and the inductance matrix $\tilde{\mathrm{L}}$ will remain positive semidefinite. Ellipsoidal (equipotential) shells are expected to suppress forward coupling, as opposed to cylindrical ones. Therefore, as orthogonal networks cover a major part of interconnects which exhibit inductance effects in the first place, i.e. data, clock, and supply lines, further exploration of the merits of the various shell types seems warranted.

Design methodologies are directed towards minimization of inductance effects, which implies placement of return paths as close as possible to the signal line. A typical example is the upcoming interest for the use of coplanar interdigitated signal/ground lines. In this respect the ability to define partial inductances in terms of magnetic fluxes extending no further than only a small fraction of the overall chip dimensions will gain importance in modelling of inductance effects in future generation VLSI designs.

Acknowledgements

AJD was supported by ESPRIT Project No. 24.115 (ACE). This work was also supported by the Dutch Technology Foundation (STW).

References

[1] A. E. Ruehli, "Inductance calculations in a complex integrated circuit environment," *IBM J. Res. Develop.*, vol. 16, pp. 470–481, 1972.

[2] M. Kamon, M. J. Tsuk, and J. K. White, "Fasthenry: A multipole-accelerated 3-d inductance extraction program," *IEEE Trans. Microwave Theory Tech.*, vol. 42, pp. 1750–1758, 1992.

[3] B. Krauter and L. T. Pileggi, "Generating sparse partial inductance matrices with guaranteed stability," in *Proc. ICCAD*, 1995, pp. 45–52.

[4] M. Beattie, L. Alatan, and L. Pileggi, "Equipotential shells for efficient partial inductance extraction," in *Proc. International Electron Devices Meeting*, 1998, pp. 303–306.

[5] F. W. Grover, *Inductance Calculations: Working Formulas and Tables*, Instrument Society of America, 1945.

[6] A.J. Dammers and N.P. van der Meijs, "Towards a sparse partial inductance matrix," in *Proc. ProRISC'98*, 1998, `http://www.stw.nl/scsi/cssp98/`.

[7] J. D. Jackson, *Classical Electrodynamics*, John Wiley & Sons, Inc., New York, 1962.